FDTD Analysis of Plane-Wave Diffraction from Microwave Devices on an Infinite Dielectric Slab

Teng-Tai Hsu, *Student Member, IEEE*, and Lawrence Carin, *Member, IEEE*

Abstract—**A 2-D (two-dimensional) Huygens surface is developed for the finite difference time domain (FDTD) algorithm, allowing the investigation of pulsed plane-wave scattering from arbitrary 2-D structures placed on or in an infinite dielectric slab. Example results are presented for scattering from a perfectly conducting strip on an infinite dielectric slab, and the results are compared with data computed via the method of moments. Additionally, the diffraction from a finite, saw-tooth dielectric grating on an infinite dielectric slab is investigated.**

I. Introduction

OVER the last several decades the use of planar transmission lines, gratings, and frequency-selective surfaces has proliferated in microwave technology. Most analyses of scattering from such structures have been performed in the frequency domain, using a variety of different numerical algorithms [1]–[4]. However, with the dramatic advances in computer speed and memory capabilities, the finite difference time domain (FDTD) has become one of the leading tools for the analysis of electromagnetic propagation and scattering [5], [6]. The FDTD has been modified recently to incorporate a periodic boundary condition [7], which is useful for modeling scattering from infinitely periodic structures. However, in many applications the device (grating, for example) is of finite size and can be modeled as situated on a dielectric substrate of infinite extent; such situations have been investigated in the frequency domain using recursive and method of moments (MoM) procedures [4]. In this letter we examine how such an analysis can be incorporated into the FDTD machinery.

II. Huygens Surface Formulation

In the FDTD, pulsed plane-wave incidence is usually simulated by using a closed Huygens surface [8], on which equivalent electric and magnetic currents are placed (because of the griding in the Yee [9] FDTD scheme, the electric and magnetic currents are actually placed on adjacent surfaces, one-half spatial cell apart). The fields inside the Huygens surface correspond to the desired incident pulsed plane wave, and these currents produce (approximately) null fields outside. For targets in free space, the equivalent currents are computed trivially from the incident field in the absence of the target; we consider here how this scheme can be modified to take into account the effects of an infinite dielectric layer.

In Fig. 1 we consider the fields due to a pulsed plane wave interacting with an infinite dielectric slab of thickness t. The bold solid lines indicate the positions of the spatially localized electric and magnetic fields, which are transverse to the direction of propagation (indicated for each wavefront by the arrows). As expected, in the air regions the fields travel at the incident angle θ_i to the normal, while inside the slab the wavefronts travel at the angle θ_t (this angle is calculated easily via transmission-line theory and is assumed constant over the pulse bandwidth; i.e., no dispersion). Additionally, the refracted wavefronts are scaled by the appropriate combination of transmission and reflection coefficients T_{ij} and Γ_{ij}, respectively, for a wavefront originating from region i and impinging on region j. We see from Fig. 1 that the refracted wavefronts reside behind the incident pulse and decay according to products of T_{ij} and Γ_{ij}. After a sufficient distance behind the incident wavefront—determined by the contrast between the impedance of the slab and the surrounding environment—the multiple refractions become negligibly small. Thus, for purposes of FDTD modeling, the equivalent Huygens surface must account for the incident pulsed plane-wave as well as a finite number of easily calculated multiple refractions. This, therefore, represents a modest escalation in the complexity of FDTD algorithms developed for free-space scattering problems.

As a demonstration of the results of such a Huygens surface, we show in Fig. 2 data for a pulsed plane wave incident on a dielectric slab of dielectric constant $\epsilon_r = 5$ and thickness $1.25\lambda_c$, where λ_c is the center wavelength of the incident pulse (shown in inset). We can clearly see the multiply refracted wavefronts in and outside the slab; further, the fields outside the Huygens surface are very small compared to those inside (theoretically they should be identically zero). In these calculations, the square grid had discretization $0.0125\lambda_c$, the temporal discretization was $0.0075\lambda_c/c$ (with c the speed of light in vacuum), and a second-order Mur [10] absorbing boundary condition was utilized. The fields outside the Huygens surface were typically 0.02% smaller than the peak of the incident pulsed plane-wave.

III. Interpretation of the Scattered Fields

Assume that the dielectric layer—in the absence of any device or perturbation—is described by the inhomogeneous,

Manuscript received June 30, 1995. This work was sponsored in part by the U.S. Air Force Office of Scientific Research under grant F49620-93-1-0093

The authors are with the Department of Electrical Engineering, Duke University Durham, NC 27708-0291 USA.

Publisher Item Identifier S 1051-8207(96)00443-6.

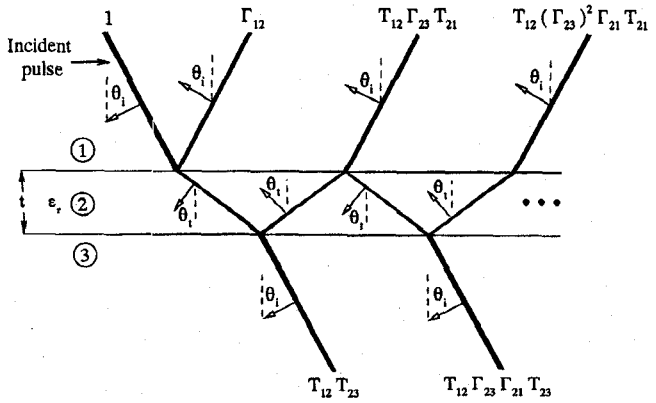

Fig. 1. Schematization of pulsed plane-wave interaction with an infinite dielectric slab of dielectric constant ϵ_r. The heavy solid lines indicate the location of the spatially (temporally) localized wavefronts, which are perpendicular to the direction of propagation (denoted by the arrows). The angle of incidence and transmission are θ_i and θ_t, respectively, and the reflection and transmission coefficients for a wavefront traveling from region i to region j are Γ_{ij} and T_{ij}, respectively.

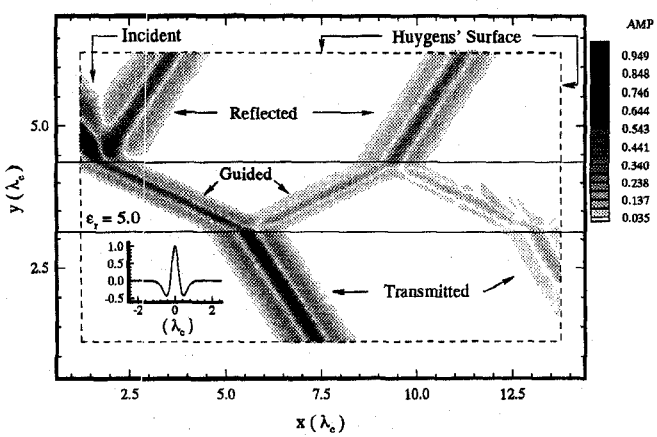

Fig. 2 Magnitude of the fields (magnitude of H_Z) for pulsed plane-wave interations with an "infinite" dielectric slab, as computed via the FDTD. The Huygens surface is shown dashed and, as expected, the incident fields outside this surface are very small (theoretically they should be zero). The shape of the incident pulse is shown inset, where the abscissa is in units of distance λ_c (λ_c represents the center wavelength of the incident pulse).

nondispersive permittivity and permeability ϵ_1 and μ_1, respectively; further, assume that $\boldsymbol{J}_i$ and $\boldsymbol{M}_i$ represent the equivalent electric and magnetic Huygens surface currents, respectively, for the incident fields. If ϵ and μ describe the inhomogeneous, nondispersive permittivity and permeability of the geometry under investigation, then the total electric and magnetic fields $\boldsymbol{E}_T$ and $\boldsymbol{H}_T$, respectively, are described by

$$\begin{aligned} \nabla \times \mathbf{E}_T &= -\mu_1 \frac{\partial}{\partial t}\mathbf{H}_T - \mathbf{M}_i - \mathbf{M}_{\mu-\mu_1} \\ \nabla \times \mathbf{H}_T &= \epsilon_1 \frac{\partial}{\partial t}\mathbf{E}_T + \mathbf{J}_i + \mathbf{J}_c + \mathbf{J}_{\epsilon-\epsilon_1} \end{aligned} \tag{1}$$

where

$$\begin{aligned} \mathbf{M}_{\mu-\mu_1} &= (\mu - \mu_1)\frac{\partial}{\partial t}\mathbf{H}_T \\ \mathbf{J}_{\epsilon-\epsilon_1} &= (\epsilon - \epsilon_1)\frac{\partial}{\partial t}\mathbf{E}_T \end{aligned} \tag{2}$$

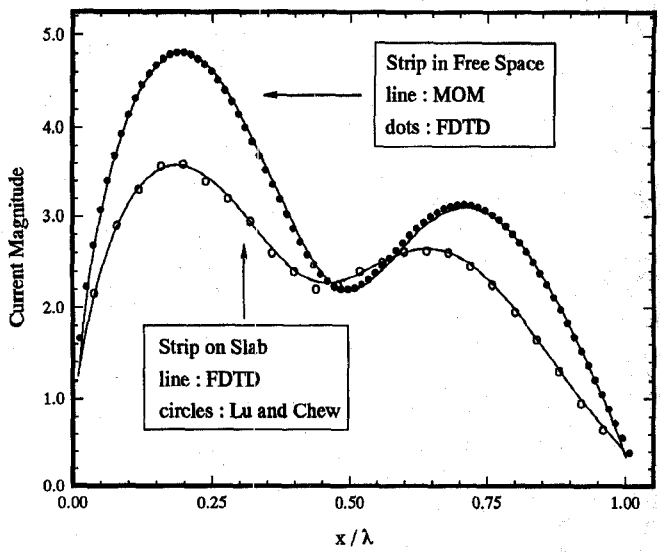

Fig. 3. Induced currents due to a plane wave incident at $\theta_i = 45^o$ upon a 1λ-wide perfectly conducting strip situated on a dielectric slab of thickness 0.1λ and $\epsilon_r = 2.1$ (λ is the free space wavelength). To demonstrate the effect of the dielectric slab, results are also shown for the strip in free space.

and $\boldsymbol{J}_c$ represents conduction currents (if any) induced by the incident signal [11]. By definition, the fields outside the Huygens surface due to $\boldsymbol{J}_i$ and $\boldsymbol{M}_i$ vanish (theoretically), and therefore the scattered fields outside this surface are approximately due to $\boldsymbol{J}_c$ and the equivalent volume currents in (2)—each of which is radiating in the presence of the dielectric slab described by ϵ_1 and μ_1; it is interesting to note that in MoM calculations, the computations are usually formulated in terms of these same currents (although usually defined in the frequency domain [12], [13]).

IV. Example Results

To calibrate the algorithm, we first consider scattering from a perfectly conducting strip on an infinite dielectric slab; this problem has been examined by Lu and Chew [1] using MoM and recursive analyses. Results are presented in Fig. 3 for the induced currents for a strip of width 1λ on a 0.1λ-thick slab of dielectric constant $\epsilon_r = 2.1$ (H_z incident at $\theta_i = 45^o$); the computations are performed in the time domain and the results in Fig. 3 were found after Fourier transform. One can see that the agreement between the FDTD results and those of Lu and Chew is excellent; for the results in Fig. 3, five multiple refractions were included for defining $\boldsymbol{J}_i$ and $\boldsymbol{M}_i$. Also shown in Fig. 3 are results for the same strip in free space and, by comparison, one can see that the dielectric loading causes a significant perturbation in the induced currents.

The final example is for a finite, dielectric-sawtooth grating situated on an infinite dielectric substrate (see Fig. 4). A pulsed plane wave is incident at $\theta_i = 45^o$ and has a temporal (spatial) shape, as shown inset in Fig. 2. The results for this example are plotted in Fig. 4 as follows. The backscattered fields outside the Huygens surface are at the bottom, the global Fourier transform of these fields is shown at the left, and the results of a short-time Fourier transform (STFT) [14] are shown in the center; the STFT utilizes a Gaussian window with standard

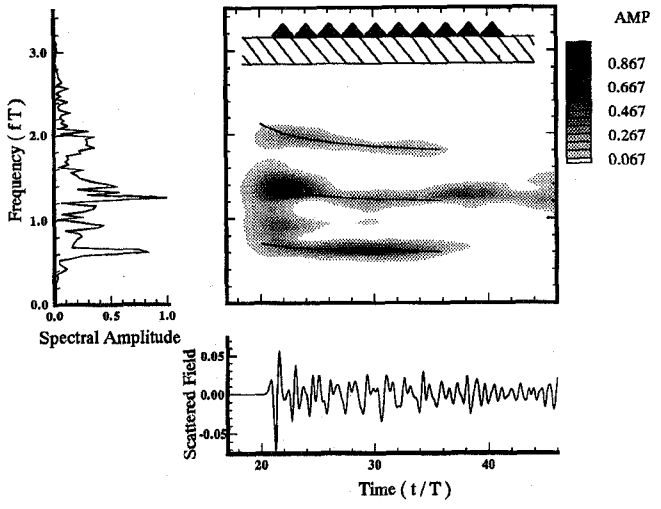

Fig. 4. Short-pulse scattering from a sawtooth dielectric grating situated on top of a dielectric slab of infinite width. The pulsed plane wave has a shape as shown inset in Fig. 2 (center wavelength $\lambda_c = 1$ cm) and the angle of incidence is $\theta_i = 45^o$. The results are plotted as follows: The scattered fields are shown at bottom, the Fourier transform of the scattered fields are shown at left, and a short-time Fourier transform of the scattered fields are shown in the center. The solid curves in the time-frequency phase space (center) described the time-dependent dispersion of the Floquet modes excited, and are given explicitly in (3). Grating parameters: the "infinite" dielectric substrate has a thickness $1\lambda_c$ and dielectric constant $\epsilon_r = 2.0$; the grating has ten dielectric sawtooth elements consisting of triangles of dielectric constant $\epsilon_r = 2.0$, height $0.25\lambda_c$, and base $1\lambda_c$ (this is also the grating period); and the fields are observed in backscatter $7.07\lambda_c$ from the right-most edge of the grating.

deviation $\sigma = 3.2T$, where $T = d/c$ (d is the grating period and c is the speed of light in vacuum). The time-frequency distribution (center of Fig. 4) demonstrates the time-dependent dispersion associated with time-domain Floquet modes; the solid curves describe the frequency dependence $\mathrm{f}_n(x,z,t)$ of the nth time-domain Floquet mode [15], [16]

$$f_n(x,z,t) = \frac{nc}{d\cos^2\theta_i} \cdot [\sin\theta_i \pm \frac{x\sin\theta_i + ct}{\sqrt{(x\sin\theta_i + ct)^2 - (z\cos\theta_i)^2}}], \quad n \neq 0. \tag{3}$$

One sees from Fig. 4 that the time-frequency distribution extracted from the scattered fields is in close agreement with the predictions in (3).

V. Conclusion

The FDTD algorithm has been modified to analyze pulsed-plane-wave diffraction from 2-D structures situated on an infinite dielectric slab. By comparing with MoM- computed data for diffraction from a perfectly conducting strip on a dielectric layer, it has been demonstrated that the FDTD results are quite accurate. To demonstrate the versatility of the algorithm, we have also considered diffraction from a sawtooth dielectric grating placed on an infinite dielectric substrate, and STFT processing has shown that the scattered fields display the time-dependent dispersion characteristic of time-domain Floquet modes. In addition to its utility for microwave devices, the technique presented here could also be modified, for example, to investigate scattering from 2-D targets buried inside a dielectric half space with surface roughness (for ground-penetrating radar applications). Finally, it should be pointed out that the results in Fig. 4 are for the near-zone of the grating; in future work we plan to develop an appropriate near-to-far-zone transformation, which will require proper use of the slab Green's function (note that this is significantly more complicated than using the free-space Green's function, as is done for investigating scattering from targets in free space [17]).

References

[1] R. Petit, Ed., *Electromagnetic Theory of Gratings*. New York: Springer-Verlag, 1980.
[2] S. D. Gedney, J. F. Lee, and R. Mittra, "A combined FEM/MoM approach to analyze the plane wave diffraction by arbitrary gratings," *IEEE Trans. Microwave Theory Tech.*, vol. 40, pp. 363–370, Feb. 1992.
[3] R. S. Chu and J. A. Kong, "Modal theory of spatially periodic media," *IEEE Trans. Microwave Theory Tech.*, vol. MTT-25, pp. 18–24, Jan. 1977.
[4] C.-C. Lu and W. C. Chew, "Electromagnetic scattering of finite strip array on a dielectric slab," *IEEE Trans. Microwave Theory Tech.*, vol. 41, pp. 97–100, Jan. 1993.
[5] K. S. Kunz and R. J. Luebbers, *The Finite Difference Time Domain Method for Electromagnetics*. Boca Raton, FL; CRC, 1993.
[6] P. G. Petropoulos, "Phase error control for FDTD methods for second and fourth order accuracy," *IEEE Trans. Antennas Propagat.*, vol. 42, pp. 859–862, June 1994.
[7] P. Harms, R. Mittra, and W. Ko, "Implementation of the periodic boundary condition in the finite-difference time-domain algorithm for FSS structures," *IEEE Trans. Antennas Propagat.*, vol. AP-42, pp. 1317–1324, Sept. 1994 (see also M. E. Veysoglu, R. T. Shin, and J.-A. Kong, "A finite-difference time-domain analysis of wave scattering from periodic surfaces: oblique incidence case," *J. Electromag. Waves and Appl.*, vol. 7, pp. 1595–1606, 1993).
[8] D. E. Merewether, R. Fisher, and F. W. Smith, "On implementing a numerical Huygens surface in a finite difference program to illuminate scattering bodies," *IEEE Trans. Nucl. Sci.*, vol. NS-27, pp. 1829–1833, Dec. 1980.
[9] K. S. Yee, "Numerical solution of initial boundary value problems involving Maxwell's equations in isotropic media," *IEEE Trans. Antennas Propagat.*, vol. AP-14, pp. 302–307, May 1966.
[10] G. Mur, "Absorbing boundary conditions for the finite-difference approximation of the time-domain electromagnetic field equations," *IEEE Trans. Electromag. Compat.*, vol. EMC-23, pp. 377–382, Nov. 1981.
[11] R. F. Harrington, *Time-Harmonic Electromagnetic Fields*. New York: McGraw-Hill, 1961, pp. 125–127.
[12] J.-F. Kiang, S. M. Ali, and J. A. Kong, "Integral equation solution to the guidance and leakage properties of coupled dielectric strip waveguides," *IEEE Trans. Microwave Theory Tech.*, vol. 38, pp. 193–203, Feb. 1990.
[13] R. F. Harrington, J. R. Mautz, and Y. Chang, "Characteristic modes for dielectric and magnetic bodies," *IEEE Trans. Antennas Propagat.*, vol. AP-20, pp. 194–198, Mar. 1972.
[14] L. Carin and L. B. Felsen, "Wave-oriented data processing for frequency and time domain scattering by nonuniform truncated array," *IEEE Trans. Antennas Propagat. Mag.*, June 1994.
[15] ——, "Time-harmonic and transient scattering by finite periodic flat strip arrays: Hybrid (ray)-(floquet mode)-(MoM) algorithm and its GTD interpretation," *IEEE Trans. Antennas Propagat.*, vol. 41, pp. 412–421, Apr. 1993.
[16] T.-T. Hsu, "Frequency and time domain analysis and signal processing of waves scattered from finite arrays," Ph.D. dissertation, Polytechnic Univ., 1995.
[17] A. Taflove and K. Umashankar, "Radar cross section of general three-dimensional scatterers," *IEEE Trans. Electromag. Compat.*, vol. EMC-25, pp. 433–440, Nov. 1983.